Increasing Fatigue LIfe of 09Mn2Si Steel by means of High-Temperature Multistep Helical Rolling

I V Vlasov[1], N S Surikova[1], S V Panin[1,2], A V Yakovlev[2] and J F Gomorova[1]

[1]Institute of Strength Physics and Materials Science SB RAS, 2/4, pr. Akademicheskii, Tomsk, 634055, Russia
[2]National Research Tomsk Polytechnic University, 30, Lenin Avenue, Tomsk, 634050, Russia

E-mail: viv@ispms.tsc.ru

Abstract. The effect of high temperature helical rolling (HR) on structure and fatigue life of 09Mn2Si pipe steel has been studied. With the use of transmission electron microscopy there was revealed that rolling gives rise to refinement of ferrite grains and cracking (fracturing) of cementite plates within the pearlite phase. The effect manifests itself to the greatest extent in the surface layer where due to the rolling the level of plastic deformation was the highest. Data of microhardness measurements confirms the gradient pattern of strain hardening over the cross section during the HR occurs while the most intensive microhardness increasing take place at the depth of up to 3 mm. According to the mechanical testing results the helical rolling of 09Mn2Si steel gives rise to increasing the level of deforming stress at the yield plateau as well as the proportionality limit with a general decrease in the relative elongation. At the same time, despite the strain hardening resulting from the helical rolling the mechanisms of plastic deformation which manifest themselves in the form of parabolic hardening with a smooth decrease in the flow stress level after neck formation are preserved in the steel. During the cyclic tension the number of cycles prior to failure increases from 2.5 to 3.8 times that depends on the location of specimens' cutting from the rolled rod. The highest improvement in fatigue fracture resistance is registered for specimens cut out from the core of the rolled rods.

1. Introduction

Development of new technologies sets new requirements to the properties of structural materials. One of the effective methods for increasing the strength properties of already developed steels is the formation of certain structural-phase states in the bulk material [1, 2]. Their variation at the processing stage allows one to obtain the required values of hardness, strength, ductility, and crack resistance. Most often such treatment includes thermal component for the formation of desired phases and subsequent plastic deformation for the purpose of additional strain hardening. Low-alloyed low-carbon ferrite-pearlite steels are most treatable with these types of processing. Violation of processing conditions or improperly selected temperature parameters can give rise to a highly stressed state usually accompanied by embrittlement of material. In this regard, it is relevant to find out complex thermal-mechanical treatments in order to attain high strength while maintaining sufficient ductility. For this purpose, high-temperature helical rolling can be utilized, which makes it possible to exert a controlled multistage thermal-mechanical impact on the material processed [3].

The main point of high-temperature multistep helical rolling is a gradient-like structure modification in the bulk material [4]. In doing so, the macroscopic structure is formed ensuring increased strength in the surface layer and maintains high ductility in the core. Preliminary established temperature and strain of helical rolling regimes [5] (including the number of passes) allow one to form a multi-level structure with high dissipative properties in the bulk material. This makes it possible to effectively suppress plastic flow localization and significantly hinder nucleation and propagation of cracks.

Low-alloyed structural 09Mn2Si steel which is widely used both at constructing pipelines as well as for manufacturing structural components was taken as an object of study. The paper is aimed at research of the impact of the helical rolling (HR) on the structure and fatigue properties of this steel.

2. Experimental

High-temperature multistep helical rolling of steel with gradual decreasing rolling temperature at each subsequent pass was performed with the help of a three-roll laboratory scale rolling machine RSP "14-40" in the temperature range 1123-773 K (850-500 °C). After each rolling pass the rod was quenched in cold water. The total degree of true logarithmic strain of the steel during the rolling was 0.8 (relative strain 73.93 %).

Dog-bone shape specimens with a gauge length of 16 × 3 × 1 mm were cut out from the rods along the longitudinal direction by the electro-spark machine. Static tension tests were carried out with the use of an Instron 5582 electromechanical testing machine; the tensile loading rate was 0.6 mm/min.

The fatigue tests were conducted with the use of Biss UTM 150 servo-hydraulic frame. In the paper, for the crack growth diagrams as well as photographs depicting their development the results are given being most close to the average ones for each group. The fatigue ratio R was set at 0.1 with the maximum load per cycle of 290 MPa and the loading frequency of 20 Hz. To localize the processes of fatigue crack nucleation, the I-shaped notch with the length of 400 μm and a tip radius of 125 μm was introduced in the middle part of each specimen.

The size of ferrite grains was measured according to ASTM E 112-96. Microhardness measurements were conducted with the help of a PMT-3 instrument with the load on the Vickers pyramid of 0.98 N (100 g). Fine crystalline structure was examined over thin foils with the use of a transmission electron microscope CM-12 (Philips) at the accelerating voltage of 200 kV.

3. Results

3.1. *Metallography.* As-received 09Mn2Si steel possesses a ferrite-pearlite structure (Figure 1, a). After the rolling, a finely dispersed structure consisting of ferrite as well as fractured plates of the pearlite phase is seen in the surface layer both along the longitudinal and transverse directions (Figure 1, b). At the depth above 1 mm in a longitudinal direction, some individual ferrite grains become visible (Figure 1, c). They have been kept undamaged by the rolling induced deformation and are elongated towards the longitudinal direction with a slight deviation to the center of the rod.

At observation in the transverse direction such grains appear as equiaxed light phases, sometimes slightly elongated (due to lateral deviations). With approaching to the rod center an increase of the size and the number of distinguishable elongated ferrite grains becomes evident, while at the distance of 4 mm their texture becomes clearly visible (Figure 1, d).

At this depth (at observation in the transverse direction) both the ferrite and pearlite phases become distinguishable. However, the helical rolling induced deformation governs poor appearance of pearlite interlayers located between ferrite grains. However, in the as-received state steel these phase boundaries look more “ragged” (caused by mixing of phases during the helical rolling).

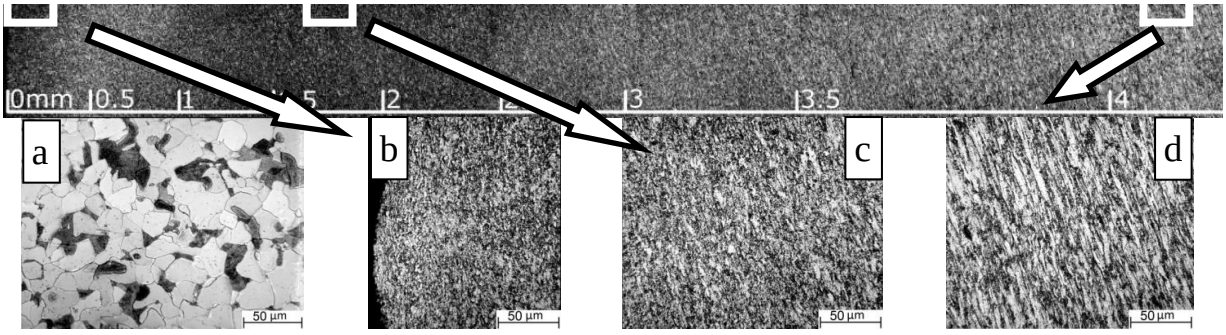

Figure 1. Optical images of the microstructure of (a) as-received steel specimen; and (b-d) after the helical rolling: longitudinal section.

3.2. *Transmission electron microscopy.* With the help of the transmission electron microscope the fine structure of the as-received steel as well as one after the HR have been studied (Figure 1, a, b). Characteristic cementite plates with a thickness of 100-150 nm are seen within the pearlite grain of the steel not subjected to the rolling. There are carbide inclusions with the size of 250-400 nm within the ferrite phase (Figure 1, a). During the rolling, refinement of ferrite grains and fracture of cementite plates has occurred (Figure 1, b). The average subgrain size of the rolled steel is about 300 nm, while in the surface layer it can reach 100 nm.

3.3. *Mechanical properties.* The microhardness over the cross section of the rod after the HR was measured (Figure 1, c). The highest degree of the microhardness increase is registered in the surface layer up to 3 mm depth, while the hardening occurs throughout the entire bulk of the rod.
Specimens for static stretching were cut out from the HR-processed rod at the depth of 3 mm where the the microhardness was lower than in the surface layer.

At the loading diagram of the as-received material one can easily distinguish a yield tooth and a yield plateau being characteristic for low carbon steels (Figure 1, d, table 1). The diagram exhibits a long stage of parabolic hardening and high value of relative elongation at break. Despite the increase in the microhardness, at the loading diagram for the HR-treated steel both the yield tooth and the yield plateau present indicating that the strain hardening mechanisms (which is of particular importance under impact loading) are kept. At the same time, the stresses at the yield point as well as the proportionality limit have increased by 26 %. Also, the stress at the yield tooth is comparable with the value of tensile strength. The duration of the yield plateau has increased by 3 times.

Table 1. Results of static tension tests.

State	Proportionality limit (MPa)	Flow stress at yield plateau (MPa)	Upper yield point (MPa)	Ultimate strength (MPa)	ε (%)
Initial state	163±10	297±10	307±20	443±20	32±3
After HR	219±10	403±20	431±20	438±20	21±3

The fracture of the HR-treated steel specimens after the neck formation occurs smoothly, much like to as-receive steel. The fact of keeping plasticity mechanisms at the yield plateau stage and the smooth failure pattern after the neck formation (with quite manifested strain hardening) can be explained by the decrease of the grain size and texture formation during the rolling. The newly formed extended grain boundaries prevent the plastic deformation development, while the ferrite grains that avoid significant hardening favouring accumulation of defects. That is why they are responsible for presence

of the yield tooth and plateau at the loading diagram. It should also be noted that the hardening of the material after the helical rolling still gives rise to the decrease of the relative elongation value (by 34 %).

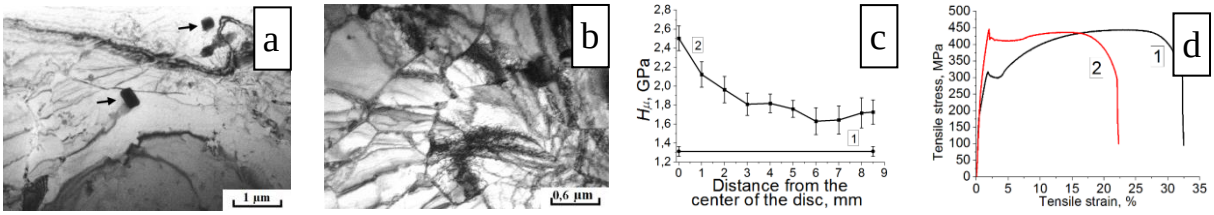

Figure 2. TEM-microimages of fine structure a) as-received (1); b) after the HR (2); c) cross-section microhardness graph in the rod as a function of distance from the surface; d) loading diagram.

Fatigue tests were carried out for the as-received 09Mn2Si steel specimens and ones after the HR. Since the rolled rod had a gradient structure over the cross section the specimens were cut out from three different locations of the rod's cross section (Figure 3, a).

It was revealed that the high-temperature helical rolling gives rise to increasing fatigue life at least by 2.5 times (table 2). Depending on the location of the specimens cutting the number of cycles prior to failure changes. The lowest increase in fatigue life after the HR is observed for specimens cut out from the area 1 where microhardness has increased to the maximum extent. Specimens from the core of the rod being characterized by the lower microhardness (as compared with specimen from the area 1) showed the largest number of cycles prior to failure. As compared to the as-received steel the number of cycles prior to fracture for the area 3 specimens have increased by 3.8 times.

Based on the results of a quantitative image analysis of the specimen surface taken during cyclic testing some graphs of the main crack opening were constructed (Figure 3, b). The calculation of the crack opening value was initiated from the moment when its length reached 80 μm (to provide the reliability of the measurement results at the used magnification of the optical surface photo observation). One can see intensive crack growth over the entire measurement range in the as-received steel that is associated with a higher ductility and lower strength of the material. For the HR case the intensive crack growth is observed mainly at the final stage of cyclic loading ($N/N_{\text{failure}} > 90$ %).

Also, for the aim of quantitative comparison of fatigue fracture regularities for various specimens the graphs of their elongation during cyclic loading were constructed (Figure 3, c). It is seen that the lowest elongation is typical for a specimen cut out from area 1. The elongation is slightly greater for a specimen taken from area 2, while the largest one is typical for the specimens cut out from area 3 which is comparable to the elongation for the as-received steel (curve 4).

Thus, the key effects identified here are: 1) in terms of the current number of cycles normalized over the total one prior failure, a macrocrack nucleates at approximately the same time; although in absolute terms the HR significantly delays the beginning of the main crack propagation stage. 2) crack opening in the as-received steel occurs at significantly higher velocity as compared to the HR specimens cut from locations 1–3; 3) the value of elongation during cyclic loading as well as the velocity of this process in the specimen cut out from zone 3 are almost identical. This indicates a high ductility of the formed structural-phase state combined with high strength properties.

The image analysis of the specimen's surface during cyclic loading (Figure 4) was carried out. The number of cycles was determined for the instance when a main crack nucleates. It can be seen that for the as-received steel (Figure 4, a-d), the value of $N_{\text{cr.init.}}/N_{\text{fail}}$ is equal to 30 % (table 2). This is characteristic of ductile steels when the duration of the main crack propagation stage significantly exceeds that of its nucleation. After the main crack has formed a manifested contraction in the notch region is seen (Figure 4, b). Subsequently, in the front of the crack tip a two-pestle like plastic deformation zone being traditional for ductile materials is formed (Figure 4, c). Its size increases with the crack growth, and is decorated with a pronounced initial grain structure of the material. The crack branches up during growth and plastic deformation, especially in the last stages, manifests itself to the greatest extent (Figure 4, d).

The specimens after the HR taken from location 1 possess the lowest value (20%) of the $N_{cr.init.}/N_{fail}$ parameter (table 2). By the authors' opinion the pointed result is associated with a high degree of strain hardening of the material in this region since due to significant defect density the crack nucleates quite early (but only with respect to the normalized number of cycles prior failure).

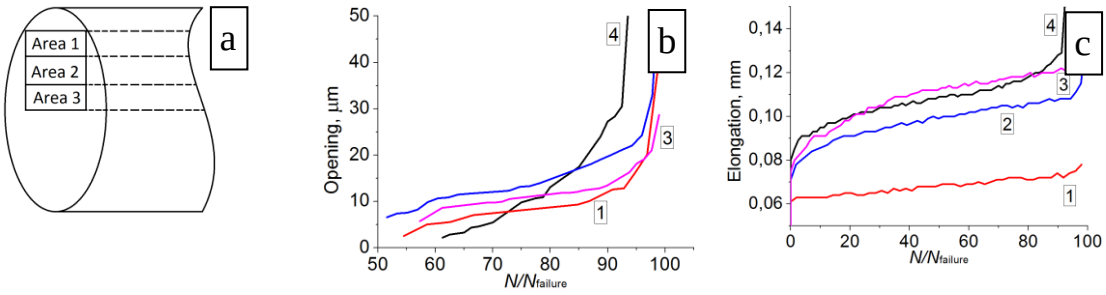

Figure 3. a) scheme of the rod and locations for cutting out specimens; b) crack opening graph; c) elongation during cyclic loading; 1) after the HR, area 1; 2) area 2; 3) area 3; 4) as-received state.

Table 2. Results of fatigue tests.

State	Area	The number of cycles to failure	$N_{cr.init.}/N_{fail}$ (%)
Initial state	-	80 000±5 000	30±4
After HR	Area 1	200 000±10 000	20±2
	Area 2	225 000±12 000	30±3
	Area 3	305 000±15 000	45±5

After the nucleation of the main fatigue crack (Figure 4, f) there are no pronounced traces of contraction, while the crack grows without branching and with minimal evidences of plastic deformation development (Figure 4, g). At the final stage, some step-like lines are formed near the main crack, being oriented towards the direction of its growth (Figure 4, h) thereby forming slight contraction. However, in comparison with as-received steel much more brittle fracture pattern is observed, while plastic deformation at the final stage is slightly pronounced. According to the authors opinion, this effect is associated with the formation of finely dispersed grain structure during the HR, when numerous boundaries of the structural elements occur impeding the main crack growth.

The highest value of the parameter $N_{cr.init.}/N_{fail}$ is observed in the specimens cut from the location 3 which is equal to 45 %. This ratio is more typical for less ductile materials, and more than 2 times differs from that for higher strength specimens cut out from the zone 1. There are no evidences of plastic contraction at crack initiation. The main crack branches during its propagation and weak traces of plastic deformation development are visible near its tip. At the final stage of crack growth slight contraction is also registered. According to the authors' opinion, the maximum increase in the fatigue life of specimens cut out from zone 3, is caused by the following reason. During the HR, quasi-laminate (textured) structure is formed in zone 3. In doing so, a fatigue crack growths towards the direction of the preferred orientation of its structural elements. In this case, the density of defects formed during the HR as compared to zone 1 is lower (as evidenced from the microhardness measurements).

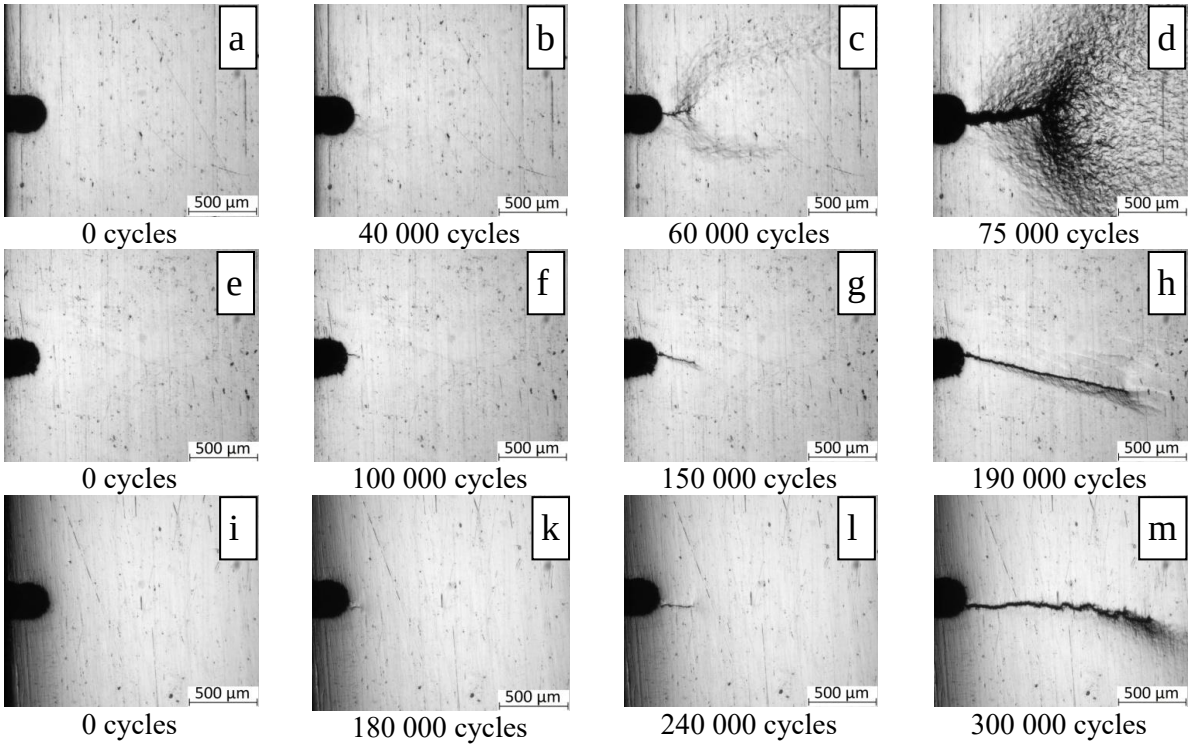

Figure 4. Images of specimens surface under cyclic tension; a) - d) as-received state; e) - h) after the helical rolling (area 1); i) - m) after the helical rolling (area 3).

As a result of the strength increase for specimens taken from zone 3, the parameter $N_{cr.init.}/N_{fail}$ has a maximum value (by the way, it gradually increases when moving from zone 1 (20 %) to the zone 2 (30 % which corresponds to the as-received steel) and then to the zone 3 (45%)). Thus, from the optimality point of view (of the gradient structure formation over the cross section), it is the material in zone 3 that should be considered as one having the best structural–phase state.

Conclusion

The structure and mechanical properties of 09Mn2Si steel were studied after the high-temperature five-step HR. It was revealed that the rod treatment results in finely dispersed structure formation in the surface layer up to 3 mm deep being caused by intensive plastic deformation. This is accompanied with fibrous-like textured structure formation consisting of thin ferrite grains elongated towards the rolling direction in the underlying layers. The greatest increase in microhardness is observed in the surface layer at the depth of up to 3 mm.

Under static tension in the HR-specimens the stress at the yield plateau as well as the proportionality limit increase by 26 %, while the tooth yield stress is comparable to the tensile strength. The duration of the yield plateau increases by 3 times. The i) preservation of the "parabolic hardening" stage, yield tooth and plateau at the tensile diagram, ii) the high level of deforming stresses, iii) the maintenance of plastic deformation mechanisms and iv) the smooth flow stress decreasing after the "neck" formation with simultaneous strain hardening are logically explained by the decrease in grain size and texture formation during the rolling including formation of numerous newly formed extended grain boundaries.

The structure of specimens cut out from various location of the rod after the helical rolling has been analyzed. It was found that the specimens taken from the core of the rod (area 3) are characterized by a more equilibrium and less deformed state that is manifested in lower microhardness, higher elongation under cyclic loading being comparable with as-received steel and more ductile pattern of the main fatigue crack growth (in comparison with area 1). Apparently, the preservation of high ductility and

the presence of the fibrous-like texture being oriented normally the direction of the crack propagation make it possible to increase the duration of main crack propagation stage while due to the increase in strength the number of cycles required for the critical accumulation of defects (the stage of the fatigue crack initiation) increases. This results in a maximum increase in fatigue life up to 3.8 times.

On the other hand, in specimens cut out from the area 1 due to the most intensive straining during the HR the highly defective structure having a lower ductility is formed. This is manifested in minimal elongation of specimens under cyclic loading and a more brittle pattern of the main crack growth. This gives rise to earlier crack nucleation ($N_{cr.init.}/N_{fail}$ =20%) and a lower number of cycles prior to failure. However, due to the strain hardening, the number of cycles prior to failure for specimens of this type remains 2.5 times higher as compared to as-received steel.

Acknowledgments
The study was performed in the framework of fundamental research Program of the Russian State Academies of Sciences for 2013–2020, line of research III.23 as well as a partial support of RFBR Grants № 18-38-00679 and 18-08-00516. Financial support of RF President grants i) Scholarship SP-2456.2019.1 and ii) RF President Council Grant for the support of leading research schools NSh-5875.2018.8 is also acknowledged.

References
[1] S S Samant, I V Singh and R N Singh 2018 *Materials Science and Engineering: A* **738** 135-152
[2] Nagaraj M and Ravisankar B 2018 *Materials Science and Engineering: A* **738** 420-429
[3] Naizabekov A, Lezhnev S, Arbuz A and Panin E 2013 *Metallurgical Research & Technology* **115**(2) 213
[4] Derevyagina L S, Gordienko A I and Kashiro P O 2019 *Russian Physics Journal* **61**(11) 1971–1977
[5] Derevyagina L S, Gordienko A I, Pochivalov Yu I and Smirnova A S 2018 *Physics of metal and mettallography* **119**(1) 83-91